Available online at www.sciencedirect.com

ScienceDirect

IFAC Papers Online CONFERENCE PAPER ARCHIVE

IFAC-PapersOnLine 48-11 (2015) 390–395

Reliable Sliding Mode Approaches for the Temperature Control of Solid Oxide Fuel Cells with Input and Input Rate Constraints

Andreas Rauh * **Luise Senkel** * **Harald Aschemann** *

* *Chair of Mechatronics, University of Rostock, Rostock, Germany (e-mail: {Andreas.Rauh, Luise.Senkel, Harald.Aschemann}@uni-rostock.de)*

Abstract: High-temperature fuel cells are promising devices to generate both electric energy and process heat in a decentralized energy supply grid. On the one hand, fuel cells have a relatively high efficiency concerning conversion of chemical energy. On the other hand, as far as solid oxide fuel cells (SOFCs) are concerned, they can also operate with a large variety of gas mixtures, involving hydrogen, methane, carbon monoxide, and carbon dioxide. This results from the fact that SOFCs are capable to perform an internal gas reformation. However, the variability of the required electric power — to be provided by the SOFC — leads to the necessity to develop reliable, real-time capable control strategies. In contrast to linear state-of-the-art approaches, these procedures should be applicable within wide ranges of operating temperatures. Moreover, the controllers have to be designed in such a way that they are robust against uncertain parameters and external disturbances. Finally, they have to guarantee that upper bounds for the admissible cell temperature are guaranteed not to be violated. For these reasons, this paper presents extensions of interval-based sliding mode controllers employing a novel barrier Lyapunov function technique. These controllers provide a way to consider one-sided state constraints as well as input and input rate constraints.

Keywords: Solid oxide fuel cells, sliding mode control, interval analysis, uncertain systems, barrier Lyapunov functions.

1. INTRODUCTION

Fuel cell systems provide a way to convert chemical energy of fuel gases directly into electric energy and — if high-temperature cells are considered — into process heat. This combined electrical and thermal power generation is one of the possibilities that are investigated for the design of flexible systems for a future decentralized power supply grid. Here, not only the advantages mentioned in the abstract of this paper have to be considered. It is also necessary to equip fuel cell systems with intelligent control approaches which allow for a non-stationary operation and for an increase of the admissible operating ranges in comparison with classical linear control approaches.

As described in (Bove and Ubertini, 2008; Huang et al., 2013; Pukrushpan et al., 2005), SOFCs are characterized by a nonlinear dynamic behavior. Generally, the system dynamics can be described by sets of partial differential equations. However, real-time capability of control and state estimation procedures impose constraints on the complexity of the applicable system models. Hence, control-oriented models, approximating the dynamics by a finite-dimensional set of ordinary differential equations (ODEs), are commonly used to design and implement feedforward and feedback controllers as well as state and disturbance observers. State-of-the-art control approaches for the thermal behavior of SOFC stack modules are mostly (gain-scheduled) PI (proportional, integral) controllers as well as linear model-predictive control techniques (Huang et al., 2013; Stiller et al., 2006). However, the applicability of these techniques requires that the operating temperature of the SOFC stack does not deviate too far from the point at which the nonlinear system model is linearized for design purposes. Moreover, classical controllers require an exact knowledge of internal parameters of the describing sets of ODEs. Both aspects are typically not fulfilled in real-life scenarios. Therefore, this paper extends interval-based sliding mode procedures (Rauh et al., 2015, 2014b) to the reliable control of SOFCs under consideration of state as well as input and input rate constraints. The state constraints are represented by one-sided limits for the maximum temperature of the individual finite volume elements in the interior of an SOFC stack. Input constraints arise from both bounded mass flows of the supplied anode and cathode gases as well as from the operating range of the available supply gas preheaters. Besides these range constraints, also input rate constraints have to be accounted for to guarantee stability and to maximize the life time of the available actuators.

This paper is structured as follows: Sec. 2 gives a brief overview of the control-oriented modeling of SOFC systems. Robust sliding mode control approaches, using fea-

10.1016/j.ifacol.2015.09.217

tures from interval analysis for handling uncertain parameters, are described in Sec. 3.1. They are extended by novel barrier Lyapunov functions in Sec. 3.2 to consider state and actuator constraints. Parameterization guidelines and strategies for gain scheduling of the controller's design parameters are described in Sec. 3.3. They aim at a reliable handling of both input and input rate constraints while proving asymptotic stability of the closed-loop system under all circumstances. Simulation results for an SOFC test rig available at the Chair of Mechatronics at the University of Rostock are summarized in Sec. 4. Conclusions and an outlook on future work are given in Sec. 5.

2. CONTROL-ORIENTED SOFC MODELING

The prerequisite for the design of reliable SOFC controllers is the modeling of the thermal behavior of the stack module. The stack module of the available test rig consists of a fixed number of planar fuel cells in electric series connection, where electric currents and gas mass flows are orthogonal to each other. In previous work (Rauh et al., 2014b), a control-oriented model was derived for the temperature distribution in the SOFC stack. The corresponding modeling approach is outlined in the following.

Firstly, it is assumed that the temperature in the interior of the SOFC stack can be approximated with sufficient accuracy by a set of ODEs. These ODEs are derived by a finite volume semi-discretization of the spatial temperature distribution. All system parameters are secondly determined experimentally either by local or global optimization procedures. Using the semi-discretization procedure, the nonlinear partial differential equation for the temperature in the interior of the SOFC stack is replaced by ODEs which assume piecewise homogeneous temperatures for each finite volume element $\mathcal{I}$ of the stack in Fig. 1.

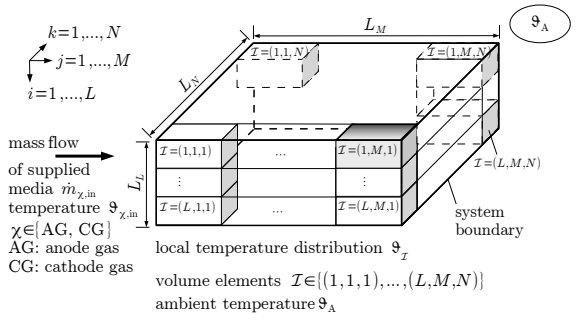

Fig. 1. Spatial semi-discretization of the SOFC stack.

During modeling, integral heat flow balances are set up for each element $\mathcal{I}$. These balance equations lead to the ODEs

$$\dot{\vartheta}_{\mathcal{I}}(t) = \frac{\dot{Q}^{\mathcal{I}}_{\mathrm{HT}}(t) + \sum\limits_{\mathrm{G}} \dot{Q}^{\mathcal{I}}_{\mathrm{G},\mathcal{I}_j^-}(t) + \dot{Q}^{\mathcal{I}}_{\mathrm{EL}}(t) + \dot{Q}^{\mathcal{I}}_{\mathrm{R}}(t)}{c_{\mathcal{I}} m_{\mathcal{I}}} \quad , \quad (1)$$

with $\mathrm{G} \in \{\mathrm{AG}, \mathrm{CG}\}$ (anode gas: AG, cathode gas: CG), where $c_{\mathcal{I}}$ is the heat capacity of the volume element $\mathcal{I}$ and $m_{\mathcal{I}}$ represents its mass parameter. The heat flow term

$$\begin{aligned}\dot{Q}^{\mathcal{I}}_{\mathrm{HT}}(t) = {} & \dot{Q}^{\mathcal{I}}_{\mathrm{HT},\mathcal{I}_i^-}(t) + \dot{Q}^{\mathcal{I}}_{\mathrm{HT},\mathcal{I}_i^+}(t) + \dot{Q}^{\mathcal{I}}_{\mathrm{HT},\mathcal{I}_j^-}(t) \\ & + \dot{Q}^{\mathcal{I}}_{\mathrm{HT},\mathcal{I}_j^+}(t) + \dot{Q}^{\mathcal{I}}_{\mathrm{HT},\mathcal{I}_k^-}(t) + \dot{Q}^{\mathcal{I}}_{\mathrm{HT},\mathcal{I}_k^+}(t)\end{aligned} \quad (2)$$

in (1) consists of heat transport between directly neighboring volume elements as well as heat transfer to the ambiance. The indices in (2) with the heat flow notation

$$\dot{Q}^{\mathcal{I}}_{\mathrm{HT},\mathcal{J}}(t) = \beta^{\mathcal{I}}_{\mathcal{J}} \cdot (\vartheta_{\mathcal{J}}(t) - \vartheta_{\mathcal{I}}(t)) \quad , \quad (3)$$

$\mathcal{J} \in \{\mathcal{I}_i^-, \mathcal{I}_i^+, \mathcal{I}_j^-, \mathcal{I}_j^+, \mathcal{I}_k^-, \mathcal{I}_k^+\}$, and the coefficient $\beta^{\mathcal{I}}_{\mathcal{J}}$ for heat conduction and convection are defined as follows: $\mathcal{I}_i^- := (i-1,j,k)$, $\mathcal{I}_i^+ := (i+1,j,k)$, $\mathcal{I}_j^- := (i,j-1,k)$, $\mathcal{I}_j^+ := (i,j+1,k)$, $\mathcal{I}_k^- := (i,j,k-1)$, $\mathcal{I}_k^+ := (i,j,k+1)$. The temperatures $\vartheta_{\mathcal{I}_i^-}(t)$ and $\vartheta_{\mathcal{I}_i^+}(t)$ denote stack temperatures for $i \geq 2$ and $i \leq L-1$. The same holds for $\vartheta_{\mathcal{I}_j^-}(t)$ and $\vartheta_{\mathcal{I}_j^+}(t)$ with $j \geq 2$ and $j \leq M-1$ and for $\vartheta_{\mathcal{I}_k^-}(t)$ and $\vartheta_{\mathcal{I}_k^+}(t)$ with $k \geq 2$ and $k \leq N-1$. In all other cases, the values $\vartheta_{\mathcal{J}}(t)$ are set to the ambient temperature $\vartheta_{\mathrm{A}}(t) = \text{const}$, where heat radiation terms are linearized locally. In addition to these internal effects, the total enthalpy flow $\sum\limits_{\mathrm{G}} \dot{Q}^{\mathcal{I}}_{\mathrm{G},\mathcal{I}_j^-}(t)$, $\mathrm{G} \in \{\mathrm{AG}, \mathrm{CG}\}$, of AG and CG is included in the ODEs, where the mass flow $\dot{m}_{\mathrm{CG}}$ and its desired temperature $\vartheta_{\mathrm{CG,d}}$ are used to design a guaranteed stabilizing control strategy that is primarily employed during the system's heating phase. Ohmic heat production $\dot{Q}^{\mathcal{I}}_{\mathrm{EL}}(t)$ and heat flows $\dot{Q}^{\mathcal{I}}_{\mathrm{R}}(t)$ due to an exothermic reaction between AG and CG conclude the energy balance. Detailed models for the local variations of the reacting gas mass flows and their temperature-dependent parameterizations are given in (Rauh et al., 2014b).

The finite volume model from (1)–(3) is coupled with the dynamics of the gas preheaters. These preheaters with corresponding mass flow controllers provide air to the cathode and a mixture of hydrogen (H_2), nitrogen (N_2) and water vapor (H_2O) to the anode, both with controllable temperature levels. As shown in (Rauh et al., 2014b), it is essential to account for the preheater dynamics during the control design for non-stationary operating conditions to avoid unnecessary chattering of the system inputs.

According to an experimental identification (Senkel et al., 2013), each preheater is described by two first-order ODEs

$$T_{\mathrm{G}} \cdot \dot{v}_{\chi}(t) + v_{\chi}(t) + \tilde{d}_{\chi}(t) = v_{\chi,\mathrm{d}}(t) = \vartheta_{\chi,\mathrm{d}}(t) \cdot \dot{m}_{\chi,\mathrm{d}}(t) \quad (4)$$

and

$$\begin{aligned}& T_{\mathrm{SL,G}} \cdot \frac{\dot{v}_{\chi,\mathrm{in}}(t)}{L \cdot N} + \frac{v_{\chi,\mathrm{in}}(t)}{L \cdot N} = \frac{v_{\chi}(t)}{L \cdot N} = \frac{\vartheta_{\chi}(t) \cdot \dot{m}_{\chi}(t)}{L \cdot N} \quad , \\ & v_{\chi,\mathrm{in}}(t) := \vartheta_{\chi,\mathrm{in}}(t) \cdot \dot{m}_{\chi,\mathrm{in}}(t), \ \dot{m}_{\chi,\mathrm{d}} = \dot{m}_{\chi} = \dot{m}_{\chi,\mathrm{in}} \quad ,\end{aligned} \quad (5)$$

with the time constants T_{G} for the subsidiary temperature control and $T_{\mathrm{SL,G}}$ for the lag behavior due to transport phenomena in the gas supply lines (SL) between the preheaters and the SOFC stack. In (4) and (5), the desired preheater temperatures (index d; serving as control inputs in addition to the desired mass flows $\dot{m}_{\mathrm{G,d}}$) are given by

$$\vartheta_{\chi,\mathrm{d}}(t) = \begin{cases} \vartheta_{\mathrm{AG,d}}(t) & \text{for } \chi \in \{\mathrm{H_2}, \mathrm{N_2}, \mathrm{H_2O}\} \\ \vartheta_{\mathrm{CG,d}}(t) & \text{for } \chi = \mathrm{CG} \end{cases} . \quad (6)$$

Because the AG components H_2, N_2, H_2O are mixed before entering the preheater, all components of the AG have one temperature in the interior of the preheater and one in the AG supply line. Analogously, the temperatures at the preheater outlets are denoted by $\vartheta_{\chi}(t)$, while the temperatures at the inlet gas manifold of the SOFC stack are given by $\vartheta_{\chi,\mathrm{in}}(t)$. In good accuracy, it can be assumed during modeling that the AG and CG mass flows can be changed instantaneously. This leads to the definition of *virtual* control signals $v_{\chi,\mathrm{d}}(t)$ in (4). Integrator disturbance models $\dot{\tilde{d}}_{\chi}(t) = 0$ are finally included in the description of the